

Development of a wearable ultrasound transducer for sensing muscle activities in assistive robotics applications: *In vivo* study

1st Xiangming Xue

*Joint Department of Biomedical Engineering
North Carolina State University
Raleigh, NC, USA
xxue5@ncsu.edu*

2nd Bohua Zhang

*Department of Mechanical and Aerospace Engineering
North Carolina State University
Raleigh, NC, USA
bzhang19@ncsu.edu*

3rd Sunho Moon

*Department of Mechanical and Aerospace Engineering
North Carolina State University
Raleigh, NC, USA
smoon4@ncsu.edu*

4th Guo-Xuan Xu

*Department of Biomedical Engineering
National Cheng Kung University
Tainan, Taiwan
P86094187@gs.ncku.edu.tw*

5th Chih-Chung Huang

*Department of Biomedical Engineering
National Cheng Kung University
Tainan, Taiwan
cchuang@mail.ncku.edu.tw*

6th Nitin Sharma

*Joint Department of Biomedical Engineering
North Carolina State University
Raleigh, NC, USA
nsharm23@ncsu.edu*

7th Xiaoning Jiang

*Department of Mechanical and Aerospace Engineering
North Carolina State University
Raleigh, NC, USA
xjiang5@ncsu.edu*

Abstract—People who suffer from the amputation of limbs or with mobility impairment due to methodological disorder sometimes require assistive robotics (AR), such as robotic prostheses and exoskeletons, to function satisfactorily and productively in daily life. Dynamic measurements of muscle voluntary activities are widely used to control AR, and sensors used to control AR should be non-invasive, effective, and wearable. Ultrasound (US) imaging is an effective method for measuring muscle activity. Nevertheless, conventional US transducers are cumbersome and inflexible, making them inconvenient for continuous monitoring of muscle activity for AR control. In light of no report available about using a flexible transducer for detecting muscle activities for AR, this work aims to develop a novel wearable US device for detecting muscle activities. In specific, a 16-element 10 MHz flexible sparse array was designed, fabricated, and characterized. The feasibility of monitoring muscle activity in different regions was demonstrated by an *in vivo* human experiment.

Index Terms—ultrasound transducers, wearable transducers, flexible transducers, muscle activities detection

I. INTRODUCTION

By 2050, the number of individuals living with amputations will double from 1.6 million in 2005 to 3.6 million [1]. Individuals with amputations, spinal cord injury (SCI), stroke, and neurologically caused mobility disorders will need assistive robotics (AR) to maintain daily quality, interaction, and productivity. AR, such as robotic prostheses and exoskeletons, are devices that integrate sensing, information processing, and perform actions for people with disabilities [2]. As opposed

to passive AR, which requires the user to change the device's ambulation mode manually, active AR uses voluntary muscle activity signals to control the device. It is generally recommended that sensors for measuring voluntary muscle activity signals be non-invasive, highly effective, and wearable to improve the functionality of AR [3].

As one of the main non-invasive techniques to represent human voluntary movement, surface electromyography (sEMG) has been explored for AR control [4]. Nevertheless, the use of sEMG has some inherent limitations, including a low signal-to-noise ratio (SNR), a lack of reliable monitoring of deeper muscles, the degradation of signal due to muscle fatigue, and muscle crosstalk [5]. Meanwhile, medical ultrasound (US) has recently been a viable alternative to sEMG for analyzing muscle activity [6]. Several limitations of sEMG in detecting muscle activity can be avoided due to the ability of US waves to penetrate deeper regions of the human body. A further advantage of US imaging is its ability to visualize and track muscle movement in real-time [7]. However, conventional US probes are bulky and may not conform to the shape of the limb. The capability of conventional handheld ultrasonic transducers to detect muscle activity is limited when the target muscle is moving rapidly. A further problem is that traditional transducers do not adhere well to the skin, which may negatively affect the accuracy of the measurement of muscle activity [8]. Therefore, conventional transducers are unsuitable for continuously monitoring voluntary effort and AR control.

In light of the advances in materials science and fabrication

We are grateful for the grants from NIH 1R21EB032059 and NSF 2124017.

techniques, the wearable US transducer can overcome several limitations associated with the traditional US, as it can be attached to the body area of interest without restricting the movement of the underlying tissues or preventing transducer shift. It has been shown recently that polymer-coated trenches in flexible silicon structures have the potential to be used for the fabrication of flexible transducers [9]. Research has also demonstrated that polymer-based structures can serve as flexible carriers for microelectromechanical systems (MEMS) sensors and piezoelectric transducers [10], [11]. Wearable US devices are becoming increasingly popular for blood pressure [12] and blood flow measurement [13], among other biomedical applications. However, no reports have been published regarding using a wearable/flexible transducer to detect muscle activity for AR. Therefore, this study aims to develop a novel wearable US device, consisting of a 4×4 PZT-5A array transducer and biomedical-grade polydimethylsiloxane (PDMS) for the substrate. Real-time analysis of forearm flexor carpi radialis (FCR) muscle activity was carried out using this array *in vivo*.

II. MATERIALS AND METHODS

A. Transducer design and fabrication

An illustration and photograph of the wearable US transducer are shown in Fig. 3 (a). In order to detect muscle movements, each element had a center frequency of 10 MHz due to the depth of penetration required. As the active layer, a piezo ceramic plate PZT-5A was mechanically diced and lapped down to achieve a thickness of 0.2 mm. The lapped active layer was attached to an acoustic matching layer with a thickness of 0.25 mm made of aluminum oxide/epoxy with a particle size of 50 nm using epoxy (EpoTek 301, Epoxy Tech. Inc., San Jose, CA, USA). On the back side of the active layer, the electrically conductive epoxy (E-Solder 3022, Von-Roll Inc., Cleveland, OH, USA) was applied as the first backing layer with a thickness of 0.28 mm. As an additional backing layer, epoxy mixed with tungsten particles was cast on top of the first backing layer.

Wearable US transducer fabrication consisted of four steps, as shown in Fig. 3 (b). In the first step, the matching layer, active layer, and two backing layers were stacked and bonded using EpoTek 301 epoxy. The bonded stacks were diced into elements of 1.4 mm lateral size as a second step. The third step is that each element was individually wired to a coaxial cable to reduce the possibility of wire damage during bending or extended motion. E-Solder 3022 epoxy was used to implement the ground connection on the electrode placed on the backside of the active layer. With conductive epoxy, the positive cable was carefully bonded to the electrode on the front side of the active layer. Upon completion of the wire connection, the elements were coated with parylene-C (SCS Labcooter, PDS 2010, SCS, Indianapolis, IN) for protection. As a final step, the fabricated elements were attached to the round 3D printed mold and arranged into a 4×4 array. The PDMS was then poured into the 3D-printed mold to create the flexible substrate. The PDMS-filled mold was then transferred to the

oven and maintained at 50 °C for six hours to complete the curing process.

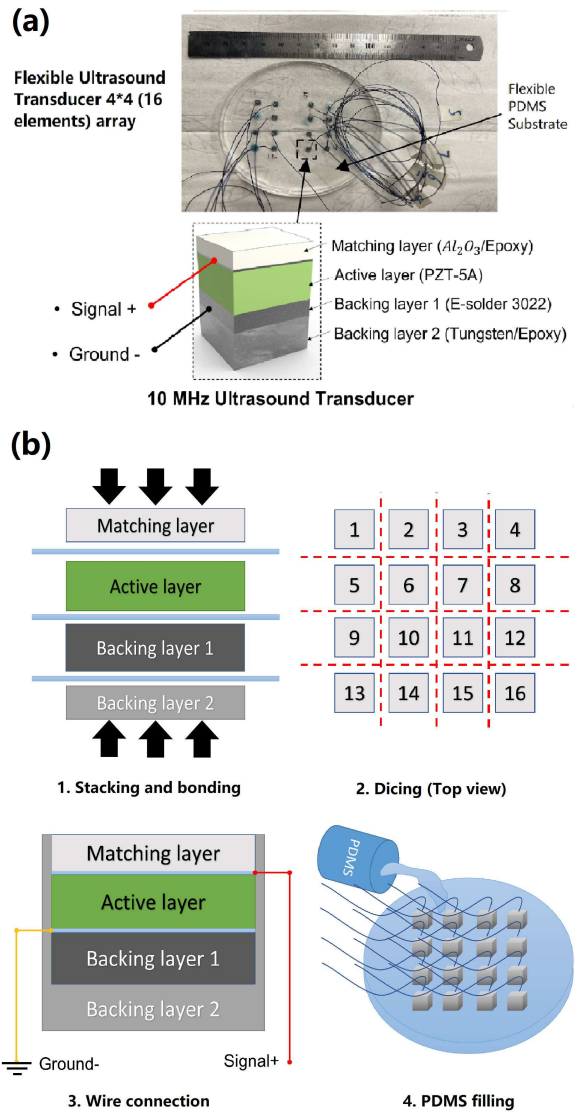


Fig. 1. (a) Schematic demonstration of the wearable US transducer design. (b) The fabrication process for the wearable US transducer

B. Transducer characterizations

The proposed transducer was characterized by pulse-echo and electrical impedance tests. An evaluation of the bandwidth and central frequency of all 16 elements of the transducer was performed by a pulse-echo test, as shown in Fig. 3 (a). Excitation of the elements was performed using a pulser and receiver (5900 PR, Olympus, WA, USA) with a pulse repetition frequency (PRF) of 200 Hz and pulse energy of 1 μ J. Echo signals were received using a bandpass filter set between 3 and 20 MHz. A steel bar was used as a reflector. An oscilloscope (DSO7104B, Agilent Technologies, Santa Clara, CA, USA) was used to capture the Radio-frequency (RF) signal. Lastly, the electric impedance, capacitance, and loss of

elements were measured with an impedance analyzer (4294A, Keysight Technologies, Santa Rosa, CA, USA). Fig. 3 (b) illustrates the setup for electrical impedance tests.

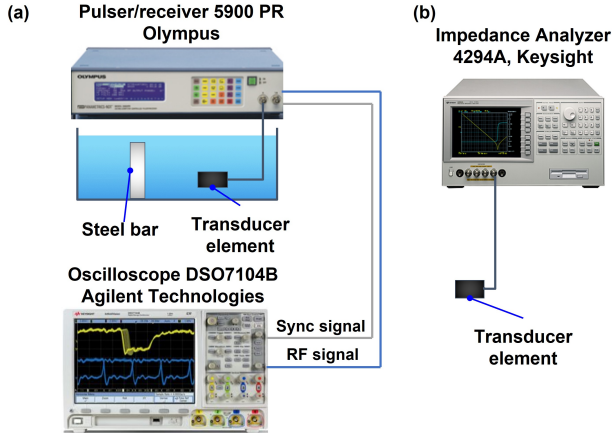


Fig. 2. Schematics of the experimental setups for transducer characterizations: (a) Pulse-echo test for the transducer; (b) Electrical impedance measurements for the transducer element

C. In vivo forearm FCR muscle activity detection experimental setup

To demonstrate the effectiveness of the proposed wearable transducer in detecting forearm FCR muscle activity in humans, an *in vivo* experiment was conducted. The experimental setup is shown in Fig. 3 (a). The subject was instructed to place his elbows on a table with his palms facing upward. The wearable transducers were attached to the subject's forearm FCR to detect muscle activity as the subject went from relaxed to clenched fist in 2.5 seconds. There were three trials conducted in total. Between every two adjacent trials, there was a 3 minutes rest to avoid muscle fatigue. The photographs of the experimental setup are shown in Fig. 3 (b).

D. RF Data Processing Procedure

The wearable transducer was driven by a customized A-mode US system with a frame rate of 500 Hz and a sampling rate of 25 MHz while the forearm was moved. All the signal and image processing were performed using MATLAB (R2020b, The MathWorks, Natick, Massachusetts, USA).

We used the RF signal at the initial relaxation location as the reference signal, and the muscle displacement was determined at 0.5 second intervals via normalized cross-correlation (NCC), a method for calculating phase differences between reference signals and comparison signals [14]:

$$NCC(t) = \frac{\sum_{n=1}^W f(n)g(n+t)}{\sqrt{\sum_{n=1}^W f^2(n) \cdot \sum_{n=1}^W g^2(n+t)}}, (t_1 \leq t \leq t_2) \quad (1)$$

where the $f(n)$ and $g(n)$ are the reference signal and comparison signal, respectively, n is the index of samples (from 1 to W), W is the window length of comparing samples, t is the time shift between the reference signal and the comparison

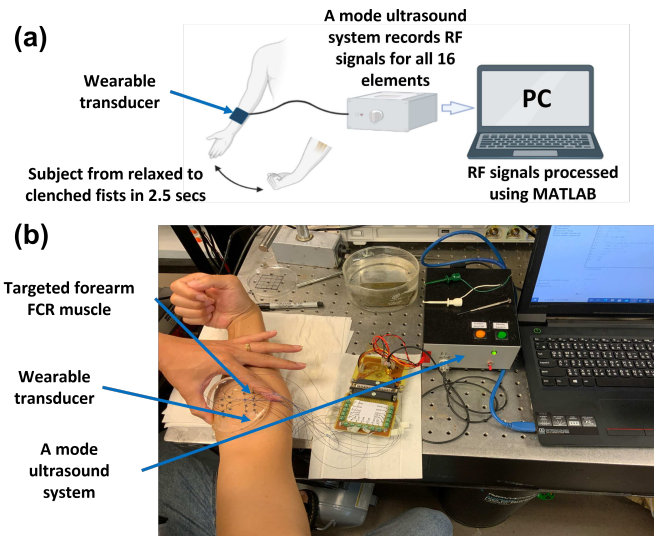


Fig. 3. Schematics of the experimental setups for transducer characterizations: (a) Pulse-echo test for the transducer; (b) Electrical impedance measurements for the transducer element

TABLE I
ACOUSTIC CHARACTERIZATIONS OF 16 ELEMENTS

Pulse-echo response test			
Property	Central frequency (MHz)	Fractional bandwidth (-6 dB)	Loop sensitivity (dB)
Average	10.78	61 %	-40
Electrical impedance test			
Property	Capacitance (@ 1 kHz, pF)	Loss (@ 1 kHz, mU)	Impedance (Ω)
Average	289.04	12.86	63.85

signal, and $[t_1, t_2]$ is the time range of interest in the reference signal.

As a result of determining the phase shifts of each element at different time steps, the relative displacements of the tissues were calculated. In order to visualize muscle movement, the relative muscle displacements were color encoded on a 4×4 matrix, which was smoothed using a linear interpolation method.

III. RESULTS

A. Transducer characterizations

Fig. 4 shows the typically measured impedance of the transducer and the pulse-echo results from element #4 as a sample. Fig. 4 (a) illustrates that the central frequency was 9.55 MHz with an impedance of 54.12 Ω . Capacitance and dielectric loss were 311 pF and 12.3 mU, respectively. The pulse-echo result for element # 4 is shown in Fig. 4 (b). The peak-to-peak amplitude was 296.6 mV with $1\mu\text{J}$ pulse energy, and the -6dB bandwidth was 84.81 %. The average characterizations for all 16 elements are presented in Table I.

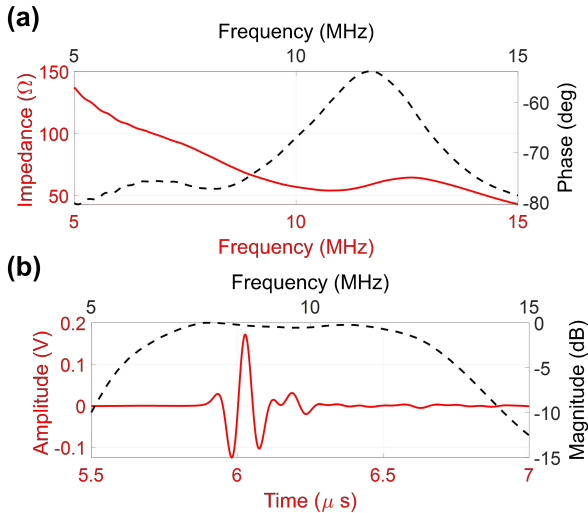


Fig. 4. Transducer characterizations results: (a) Electrical impedance magnitude (solid line) and phase plots (dashed line); (b) Time-domain pulse-echo response (solid line) and normalized frequency spectrum (dashed line) of element #4

B. In-vivo results

Fig. 5 illustrates the muscle movement imaging of forearm FCR over a range of time steps (from 0.5 seconds to 2.5 seconds). The 4×4 matrix represents the locations of 16 elements of the transducer. As shown in Fig. 5, the muscle displacements increased over time, which is consistent with the experimental setup in which the subject went from relaxed to clenched in a fist. Moreover, a larger displacement was observed in the part of the target muscle associated with the fist movement, which is represented in the color map as red. This method allows us to determine the role of a specific muscle.

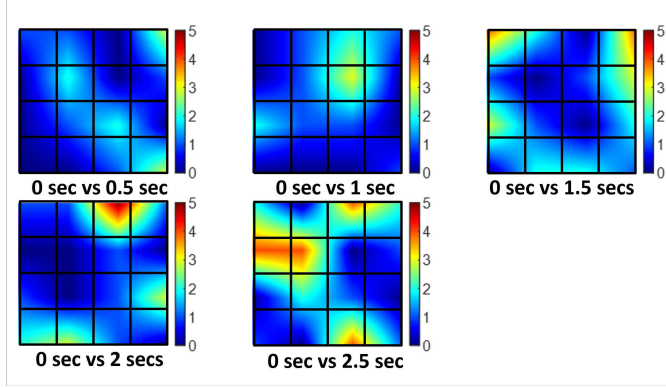


Fig. 5. Muscle average movement imaging during *in-vivo* test. The color bar represents the relative displacement of the muscle. The displacement was calculated using the forearm at relaxing as the reference

IV. CONCLUSION

In this study, the fabrication procedure for incorporating PZT-5A elements into PDMS substrates was demonstrated, resulting in a flexible and wearable US transducer array. The

4×4 array consists of 16 elements and the size of each element was $1.4 \text{ mm} \times 1.4 \text{ mm}$ with a thickness of about 1.2 mm. In average, the central frequency, the -6 dB bandwidth, and the electrical impedance were 10.78 MHz, 61 %, and 63.85Ω , respectively. *In-vivo* experiments demonstrated the feasibility of using the proposed transducer to monitor muscle activity. Muscle movement imaging was used to visualize the muscle displacement. In the future, this device could be used in motion classification and assistive robotics, due to its flexibility, wearability, and high degree of customization.

ACKNOWLEDGMENT

We are grateful for the grants from NIH 1R21EB032059 and NSF 2124017.

REFERENCES

- [1] K. Ziegler-Graham, E. J. MacKenzie, P. L. Ephraim, T. G. Travison, and R. Brookmeyer, "Estimating the prevalence of limb loss in the united states: 2005 to 2050," *Archives of physical medicine and rehabilitation*, vol. 89, no. 3, pp. 422–429, 2008.
- [2] D. P. Miller, "Assistive robotics: an overview," *Assistive technology and artificial intelligence*, pp. 126–136, 1998.
- [3] J. Lobo-Prat, P. N. Kooren, A. H. Stienen, J. L. Herder, B. F. Koopman, and P. H. Veltink, "Non-invasive control interfaces for intention detection in active movement-assistive devices," *Journal of neuroengineering and rehabilitation*, vol. 11, no. 1, pp. 1–22, 2014.
- [4] A. H. Al-Timemy, G. Bugmann, J. Escudero, and N. Outram, "Classification of finger movements for the dexterous hand prosthesis control with surface electromyography," *IEEE journal of biomedical and health informatics*, vol. 17, no. 3, pp. 608–618, 2013.
- [5] I. Talib, K. Sundaraj, C. K. Lam, J. Hussain, M. Ali *et al.*, "A review on crosstalk in myographic signals," *European journal of applied physiology*, vol. 119, no. 1, pp. 9–28, 2019.
- [6] Q. Zhang, A. Iyer, K. Lambeth, K. Kim, and N. Sharma, "Ultrasound echogenicity as an indicator of muscle fatigue during functional electrical stimulation," *Sensors*, vol. 22, no. 1, p. 335, 2022.
- [7] N. J. Cronin, R. af Klint, M. J. Grey, and T. Sinkjaer, "Ultrasonography as a tool to study afferent feedback from the muscle–tendon complex during human walking," *Journal of Electromyography and Kinesiology*, vol. 21, no. 2, pp. 197–207, 2011.
- [8] C. Castellini, G. Passig, and E. Zarka, "Using ultrasound images of the forearm to predict finger positions," *IEEE Transactions on Neural Systems and Rehabilitation Engineering*, vol. 20, no. 6, pp. 788–797, 2012.
- [9] K.-I. Jang, S. Y. Han, S. Xu, K. E. Mathewson, Y. Zhang, J.-W. Jeong, G.-T. Kim, R. C. Webb, J. W. Lee, T. J. Dawidczyk *et al.*, "Rugged and breathable forms of stretchable electronics with adherent composite substrates for transcutaneous monitoring," *Nature communications*, vol. 5, no. 1, pp. 1–10, 2014.
- [10] X. Zhuang, D.-S. Lin, Ö. Oralkan, and B. T. Khuri-Yakub, "Fabrication of flexible transducer arrays with through-wafer electrical interconnects based on trench refilling with pdms," *Journal of Microelectromechanical Systems*, vol. 17, no. 2, pp. 446–452, 2008.
- [11] T. Kim, Z. Cui, W.-Y. Chang, H. Kim, Y. Zhu, and X. Jiang, "Flexible 1–3 composite ultrasound transducers with silver-nanowire-based stretchable electrodes," *IEEE Transactions on Industrial Electronics*, vol. 67, no. 8, pp. 6955–6962, 2019.
- [12] C. Peng, M. Chen, H. K. Sim, Y. Zhu, and X. Jiang, "Noninvasive and nonocclusive blood pressure monitoring via a flexible piezo-composite ultrasonic sensor," *IEEE Sensors Journal*, vol. 21, no. 3, pp. 2642–2650, 2020.
- [13] C.-C. Huang, P.-Y. Lee, P.-Y. Chen, and T.-Y. Liu, "Design and implementation of a smartphone-based portable ultrasound pulsed-wave doppler device for blood flow measurement," *IEEE transactions on ultrasonics, ferroelectrics, and frequency control*, vol. 59, no. 1, pp. 182–188, 2012.
- [14] F. Viola and W. F. Walker, "A comparison of the performance of time-delay estimators in medical ultrasound," *IEEE transactions on ultrasonics, ferroelectrics, and frequency control*, vol. 50, no. 4, pp. 392–401, 2003.